Particle-to-Bubble Adhesion in Gas/Liquid/Solid Slurries

H. Vinke, P. J. Hamersma, and J. M. H. Fortuin
Dept. of Chemical Engineering, University of Amsterdam, 1018 WV Amsterdam, The Netherlands

In gas/liquid/solid slurries, adhesion of small particles to gas bubbles is often encountered, for example, during flotation of finely divided minerals and in slurry reactors where particle-to-bubble adhesion may result in an enhanced gas absorption rate (Wimmers, 1987; Lindner, 1988). The adhesion of small particles to gas bubbles in water is studied with a modified bubble pick-up method. The extent of the particle-to-bubble adhesion is revealed in the angle α_{max}, by which the gas-bubble surface is covered by adhering particles under static conditions. It is shown that α_{max} depends on the modified Eötvös number, the ratio of the particle and bubble radii, and the effective contact angle θ_E. It is also found that θ_E is affected by the curvature of the three-phase contact ring and by the type of the gas.

A "particle-to-bubble adhesion" model, indicated by PBA model, based on a balance of forces under static conditions, is developed to calculate the value of θ_E from the measured values of α_{max}. The measured values of $\cos(\theta_E)$ appeared to be a linear function of the curvature $1/r$ of the three-phase contact ring which is in accordance with the extended Young-Dupré equation.

Introduction

In slurries, the adhesion of particles to gas bubbles is affected by the value of the gas/liquid/solid (G/L/S) contact angle θ. Several methods are available to determine the contact angle of powders experimentally (Ayala, 1987; Neumann and Good, 1979; Heertjes and Kossen, 1967; Kossen and Heertjes, 1965; Sell, 1966, 1972). A disadvantage of these methods is that the powder is treated in such a way that the structure and the curvature of the surface of the solid particles is changed, which in turn affects the value of the contact angle considerably. Moreover, these methods may not be applied in the case of porous particles and for systems with $\theta < 15°$.

The contact angle of a G/L/S system is determined considering the following factors:

- At physical equilibrium, gas adsorbed on the surface of the solids can affect the character of this surface and as a consequence the value of the contact angle.
- The contact angle, θ_0, which is considered as a transport property of the G/L/S system, generally refers to a straight three-phase contact line obtained by the intersection of two flat interfaces, such as a "flat" gas-liquid surface and a flat gas-solid surface (see Figure 1a).
- If the three-phase contact line is curved (see Figure 1b), the contact angle will have a lower value (Langmuir, 1933) in accordance with the extended Young-Dupré equation (Schulze, 1984).

In this article, the particle-to-bubble adhesion (PBA) is studied under static conditions by means of a bubble pick-up (BPU) method, which is a modification of the method used by Wimmers and Fortuin (1988). According to this method, the extent of particle-to-bubble adhesion is revealed in the angle by which a gas bubble is covered by adhering particles under static conditions. Advantages of this BPU method are: (a) no pretreatment of the particles is required; (b) it is suitable for the determination of contact angles $\theta < 15°$; (c) it can also be applied to porous particles; and (d) it is more closely related to the conditions occurring during flotation and in slurry reactors than existing methods.

A particle-to-bubble adhesion model, denoted PBA model, will be developed to calculate the value of the effective contact angle from the measured maximum angle of the bubble-surface area, covered by small porous particles in a stagnant liquid. The effect of the curvatures of the interfaces on the value of the contact angle will be taken into account.

Correspondence concerning this article should be addressed to J. M. H. Fortuin.

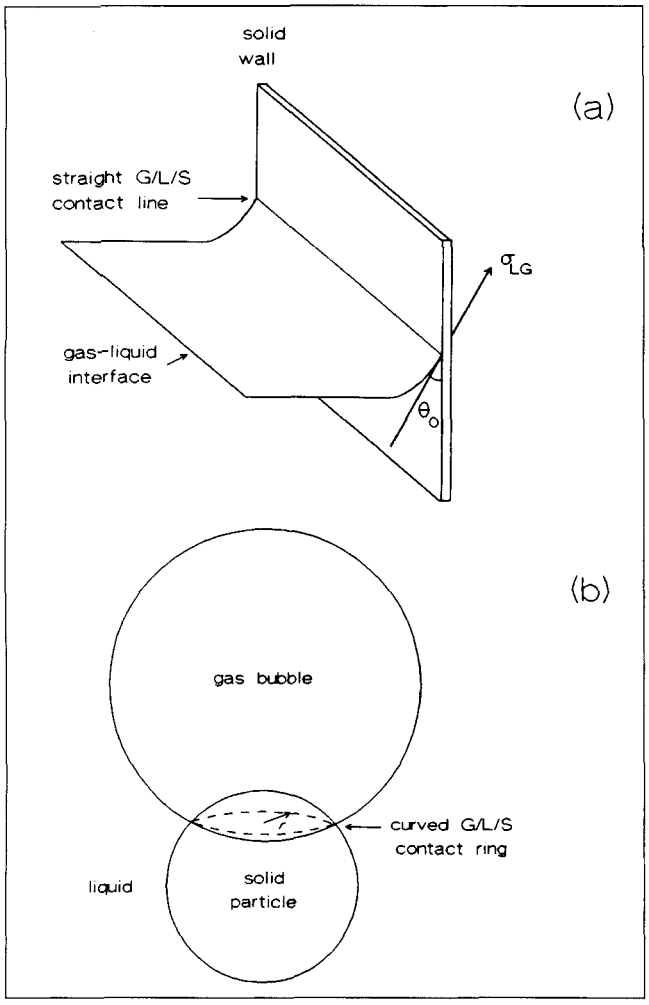

Figure 1. (a) G/L/S contact angle θ_0 at a straight G/L/S contact line occurring at the intersection of a flat gas-liquid surface and a flat solid wall; (b) G/L/S contact angle θ affected by the curvature of G/L/S contact ring.

PBA Model

The adhesion of solid particles to a gas bubble in a stagnant liquid will be derived from a balance of three forces. The PBA model, which is based on a new concept and differs from models previously developed by Wimmers (1987) and Wimmers and Fortuin (1988), will be applied to:

- A cluster of spherical particles adhering to a gas bubble
- A gas bubble partially covered by a monolayer of adhering solid particles.

Cluster of spherical particles adhering to a gas bubble

For a cluster of particles adhering to a much larger gas bubble under static conditions (see Figure 2), it will be assumed that: (a) the cluster consists of n_C equal-sized particles; (b) one single particle (A) of the cluster which is adhering to a much larger spherical gas bubble (B) is nearly completely immersed in the liquid; and (c) the other particles (C) of the cluster, which are cohering to this single particle A, are completely immersed in the liquid.

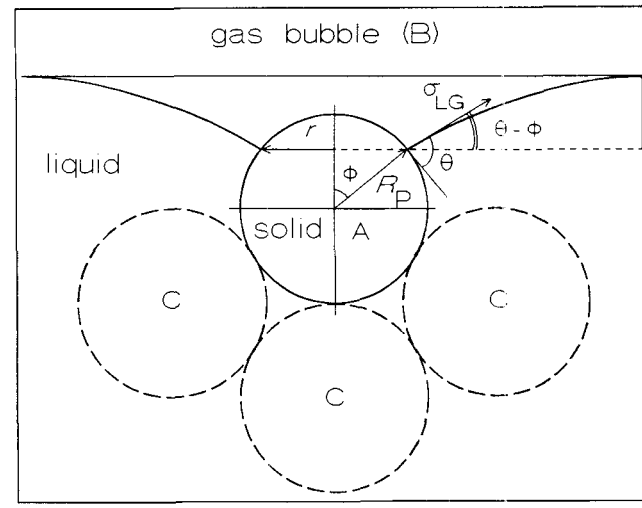

Figure 2. (A) One single particle of a cluster of equal-sized particles (C) adhering to a much larger gas bubble (B) under static conditions.

Regarding the upwardly directed forces as positive, the following three forces acting on the cluster of particles can be formulated for static conditions if $\rho_G/\rho_L \ll 1$, (Schulze, 1984):

The apparent weight of the cluster:

$$F_{AC} = n_C \cdot F_A \tag{1}$$

where

$$F_A = -\frac{4}{3}\pi R_P^3(\rho_P - \rho_L)g$$

The capillary force:

$$F_C = 2\pi R_P(\sin\varphi)\sigma_{LG}\sin(\theta - \varphi) \tag{2}$$

A force as a result of the capillary pressure in the gas bubble:

$$F_P = -P_\sigma \pi r^2 \approx -\pi R_P^2(\sin^2\varphi)(2\sigma_{LG}/R_B) \tag{3}$$

The sum of the three forces follows from:

$$\Sigma F = F_{AC} + F_C + F_P \tag{4}$$

Substituting Eqs. 1 to 3 into Eq. 4 and dividing it by the absolute value of the apparent weight $|F_A|$ of a single particle, result in:

$$\frac{\Sigma F}{|F_A|} = \frac{3}{2Eo} \cdot \{\sin(\theta - \varphi)\sin(\varphi) - \lambda \cdot \sin^2(\varphi)\} - n_C \tag{5}$$

where the modified Eötvös number and the ratio λ are defined as:

$$Eo = (\rho_P - \rho_L)gR_P^2/\sigma_{LG} \quad \text{and} \quad \lambda = R_P/R_B \tag{6}$$

Under static conditions, $\Sigma F/|F_A| = 0$ and $\varphi = \varphi_s$. As a consequence, Eq. 5 results in:

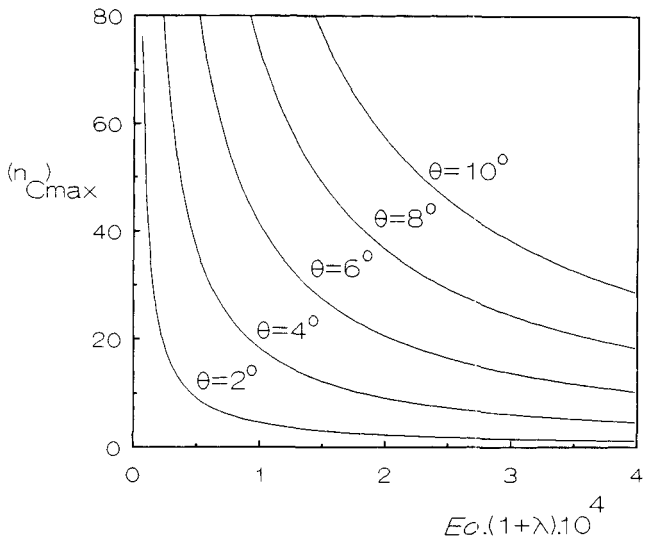

Figure 3. Relation between $(n_C)_{max}$ as a function of $Eo\cdot(1+\lambda)$ for different values of θ calculated with Eq. 11.

$$n_C=\frac{3}{2Eo}\cdot\{\sin(\theta-\varphi_s)\sin(\varphi_s)-\lambda\cdot\sin^2(\varphi_s)\} \tag{7}$$

The value of $\varphi_s=\varphi_m$, where $n_C=(n_C)_{max}$ is found from Eq. 7 and $dn_C/d\varphi_s=0$, results in:

$$\theta=2\varphi_m+\text{arc sin}\{\lambda\cdot\sin(2\varphi_m)\} \tag{8}$$

and

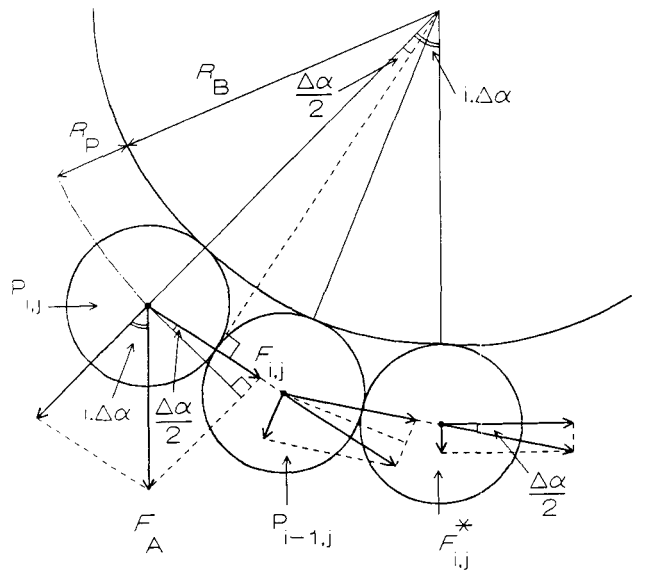

Figure 4. Vertical cross-section of a gas bubble with adhering particles.

The force $F_{i,j}$ which is a component of the apparent weight F_A of a particle $P_{i,j}$ positioned under an angle $i\cdot\Delta\alpha$, is exerted on a particle $P_{i-1,j}$ positioned under an angle $(i-1)\cdot\Delta\alpha$ and so on. For equal spherical particles, only the direction of this force changes with i but the value of this force remains constant. Particle $P_{i,j}$ positioned under an angle $i\cdot\Delta\alpha$ exerts a downward force $F^*_{i,j}$ on the lowest particle.

$$(n_C)_{max}=\frac{3}{2Eo}\cdot\{\sin(\theta-\varphi_m)\sin(\varphi_m)-\lambda\cdot\sin^2(\varphi_m)\} \tag{9}$$

For the experiments presented here, the values of θ and φ_m are small; as a consequence, $\sin(\theta-\varphi_m)\approx\theta-\varphi_m$, $\sin(\varphi_m)\approx\varphi_m$ and the following approximations of Eqs. 8 and 9 may be applied:

$$\varphi_m=\frac{\theta}{2(1+\lambda)} \tag{10}$$

and

$$(n_C)_{max}=\frac{3\theta^2}{8Eo(1+\lambda)} \tag{11}$$

The value $(n_C)_{max}$ denotes the maximum value of the ratio between the apparent weight of the cluster of particles and that of one single *adhering* particle (see Figure 2), before this particle is released from the gas bubble. In Figure 3, $(n_C)_{max}$ is plotted against $Eo\cdot(1+\lambda)$ with θ as a parameter.

From Eq. 11, it can be obtained that:

$$\theta^2=(8/3)\cdot Eo\cdot(1+\lambda)\cdot(n_C)_{max} \tag{12}$$

Adhesion of a monolayer of solid particles to a gas bubble

The adhesion of a monolayer of solid particles to a gas bubble is accomplished with the following assumptions. The adhering monolayer consists of spherical particles of equal size, which partially covers the spherical gas bubble. The lowest particle, which is positioned at the bottom of the gas bubble, carries a part of the apparent weight of other adhering particles in the monolayer. If the angle of bubble-surface coverage is maximum, the lowest particle is assumed to carry a maximum number of adhering particles, resulting in $\varphi_s=\varphi_m$. It is also assumed that: the covered part of the bubble surface is homogeneously occupied by particles; the shape of the spherical gas bubble is not changed by the adhering particle layer; and the distance between the center of the bubble and that of each particle is approximately equal to the sum of the radius R_P of the particle and R_B of the bubble. In addition, the centers of the particles are assumed to lie on a globe with radius R_P+R_B, $P_{i,j}$ is the intersection point of parallel i and meridian j of this *globe*, and $P_{0,0}$ is positioned at the bottom of the globe. The force exerted by an adhering particle on a contacting other adhering particle is also assumed to act along the line connecting the centers of these particles.

In Figure 4, a vertical cross-section of a bubble with a monolayer of adhering particles is shown. The apparent weight F_A of particle $P_{i,j}$ positioned under an angle $i\cdot\Delta\alpha$ has a component $F_{i,j}$, which is found by applying the "law of sines" and results in:

$$F_{i,j}=\frac{F_A}{\cos(\Delta\alpha/2)}\sin(i\cdot\Delta\alpha) \tag{13}$$

This force acts from the center of particle $P_{i,j}$ to the center of particle $P_{i-1,j}$ as is shown in Figure 4. Because of the geometry

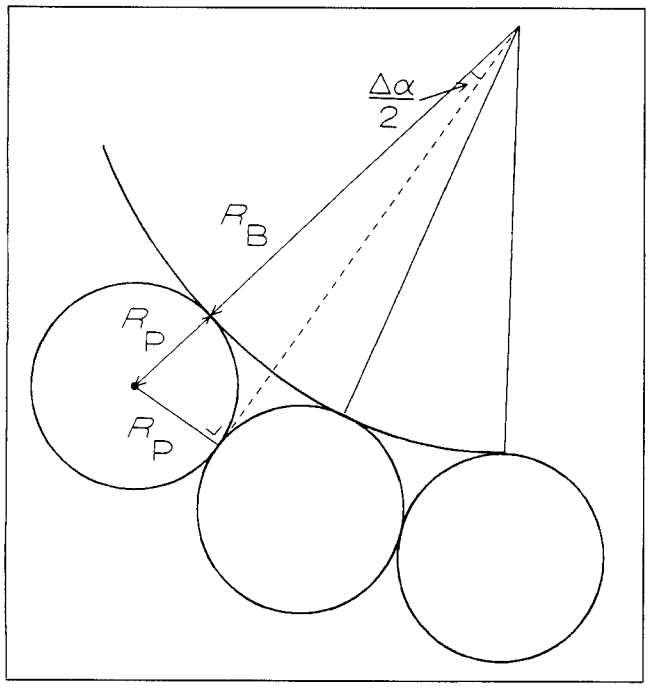

Figure 5. Vertical cross-section of a gas bubble with adhering particles.

$\sin(\Delta\alpha/2) = R_P/(R_P+R_B) = \lambda/(1+\lambda)$.

of the system considered, only the direction of force $F_{i,j}$ changes with i but its value remains constant in tangential direction. The downward force exerted by particle $P_{i,j}$ on the lowest particle is obtained from:

$$F^*_{i,j} = F_{i,j} \cdot \sin(\Delta\alpha/2) \tag{14}$$

Substitution of Eq. 13 into Eq. 14 results in:

$$F^*_{i,j} = F_A \cdot \tan(\Delta\alpha/2)\sin(i \cdot \Delta\alpha) \tag{15}$$

The number of particles positioned on parallel i can be approximated by:

$$N_i = \frac{\text{perimeter of parallel } i}{\text{diameter of a particle}} = \frac{2\pi(R_P+R_B)\sin(i\cdot\Delta\alpha)}{2R_P} \tag{16}$$

The downward force exerted on the lowest particle by all the particles positioned on parallel i is obtained from:

$$F^*_i = N_i F^*_{i,j} = F_A \cdot \tan(\Delta\alpha/2) \cdot \frac{\pi(R_P+R_B)\cdot\sin^2(i\cdot\Delta\alpha)}{R_P} \tag{17}$$

The downward force exerted on the lowest particle by the particles positioned on the parallels 1 to n is obtained from:

$$F^* = \sum_{i=1}^{n} F^*_i \tag{18}$$

Substitution of Eq. 17 into Eq. 18 results in:

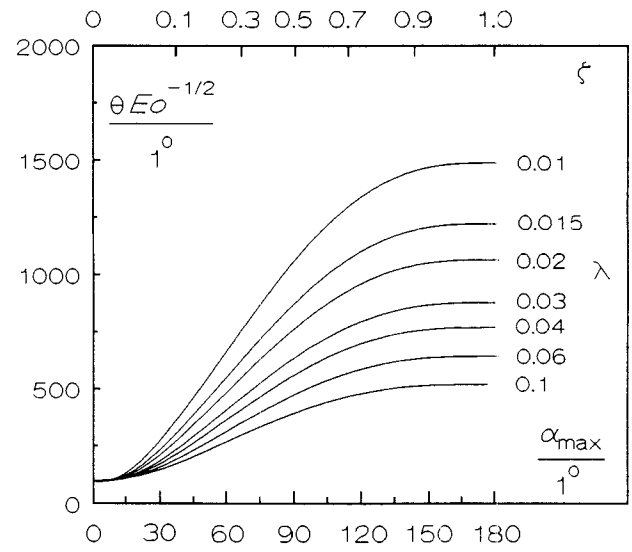

Figure 6. Value of $\theta \cdot Eo^{-0.5}$ as a function of the angle of bubble-surface coverage α_{max} with λ as a parameter (Eqs. 23 and 24).

The value of the contact angle θ can be obtained directly from the measured values of α_{max}, λ and Eo.

$$F^* = \pi F_A \cdot \tan(\Delta\alpha/2) \cdot \frac{R_P+R_B}{R_P} \cdot \sum_{i=1}^{n} \sin^2(i\cdot\Delta\alpha) \tag{19}$$

For small values of $\Delta\alpha/2$, the following approximation holds (see Figure 5):

$$\Delta\alpha/2 \approx \tan(\Delta\alpha/2) \approx \sin(\Delta\alpha/2) = \frac{R_P}{R_P+R_B} = \frac{\lambda}{1+\lambda} \tag{20}$$

Combination of Eqs. 19 and 20 results in:

$$F^* = F_A \pi \cdot \sum_{i=1}^{n} \sin^2(i\cdot\Delta\alpha) \tag{21}$$

Under static conditions, the following balance of forces acting on the *lowest* particle of the adhering monolayer of particles holds:

$$\Sigma F = F_A + F_C + F_P + F^* = 0 \tag{22}$$

Further, $\varphi_s = \varphi_m$, because F^* denotes the maximum value of the downward force exerted on the lowest particle by the other adhering particles of the monolayer. Substitution of Eqs. 1 to 3, 10, 20, 21 into Eq. 22 results in:

$$\theta^2 = (8/3)\cdot Eo \cdot (1+\lambda) \cdot \left\{1 + \pi \cdot \sum_{i=1}^{n} \sin^2[2\lambda i/(1+\lambda)]\right\} \tag{23}$$

where

$$n = \frac{\alpha_{max}}{\Delta\alpha} = \alpha_{max} \cdot \frac{1+\lambda}{2\lambda} \tag{24}$$

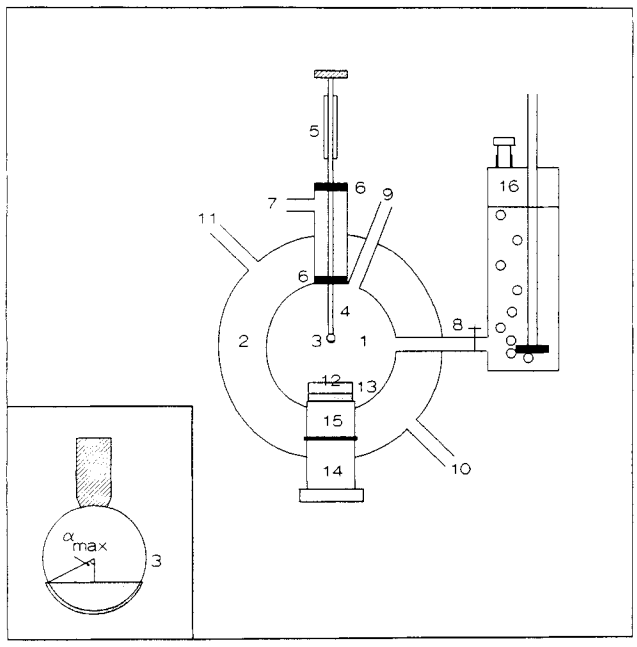

Figure 7. Bubble pick-up apparatus.

1. inner cell containing stagnant liquid; 2. outer cell used to thermostat the inner cell; 3. gas bubble with adhering particles; 4. needle; 5. gas-tight syringe; 6. rubber septums; 7. gas containing cylinder; 8. gas-saturated liquid inlet; 9. inlet through which a gas-saturated concentrated suspension of catalyst particles is added; 10. thermostatted water inlet; 11. thermostatted water outlet; 12. small glass cup; 13. layer of sedimented small catalyst particles; 14. cup holder; 15. O-type seal; 16. saturation bottle

In Eq. 24, α_{max} is the maximum angle of bubble-surface coverage which can be found under static conditions (see Figure 7, item 3).

With Eqs. 23 and 24 the contact angle θ can be calculated from the measured value of α_{max}, the modified Eötvös number of the G/L/S system and the ratio λ of the particle and bubble radii, provided that θ is small ($\theta \leq 15°$). Note that in Eqs. 23 and 24, the angles θ and α_{max} are in radians.

In Figure 6, the values of $\theta \cdot Eo^{-0.5}$, calculated with Eqs. 23 and 24, are plotted as a function of α_{max} with λ as a parameter. The value of θ can be obtained directly from α_{max}, λ, and Eo, as shown in Figure 6.

If we introduce the physical quantity:

$$(n_A)_{max} = 1 + \pi \cdot \sum_{i=1}^{n} \sin^2[2\lambda i/(1+\lambda)] \tag{25}$$

Equation 23 results in:

$$\theta^2 = (8/3) \cdot Eo \cdot (1+\lambda) \cdot (n_A)_{max} \tag{26}$$

The similarity of Eqs. 12 and 26 makes it possible to conclude that a monolayer consisting of N_A adhering particles, for example, exerts a downward force on the lowest particle, which is equal to the apparent weight of a cluster consisting of $(n_A)_{max}$ particles, where $(n_A)_{max} < N_A$.

Applications of the PBA model

The summation in Eq. 25 may be approximated by the following integration, provided that $\lambda < 0.1$:

$$(n_A)_{max} = 1 + \pi \cdot \sum_{i=1}^{n} \sin^2[2\lambda i/(1+\lambda)]$$

$$\approx 1 + \pi \cdot \frac{1+\lambda}{2\lambda} \cdot \int_0^{\alpha_{max}} \sin^2\alpha d\alpha$$

$$(n_A)_{max} \approx 1 + \frac{\pi}{4} \cdot \frac{1+\lambda}{2\lambda} \cdot (2\alpha_{max} - \sin(2\alpha_{max})) \tag{27}$$

Substitution of Eq. 27 into Eq. 26 results in:

$$\theta^2 = (8/3) \cdot Eo \cdot (1+\lambda) \cdot \left\{1 + \frac{\pi}{4} \cdot \frac{1+\lambda}{2\lambda} \cdot (2\alpha_{max} - \sin(2\alpha_{max}))\right\} \tag{28}$$

The minimum value θ^* required for complete bubble-surface coverage follows from Eq. 28 and $\alpha_{max} = \pi$:

$$(\theta^*)^2 = (8/3) \cdot Eo \cdot (1+\lambda) \cdot \left\{1 + \frac{\pi^2}{2} \cdot \frac{1+\lambda}{2\lambda}\right\} \tag{29}$$

Using Eqs. 16 and 20, the total number of adhering particles can be obtained from:

$$N_A = 1 + \sum_{i=1}^{n} N_i = 1 + 2\pi \cdot \frac{1+\lambda}{2\lambda} \cdot \sum_{i=1}^{n} \sin(i \cdot \Delta\alpha) \tag{30}$$

If the summation in Eq. 30 is approximated by an integration, Eq. 30 results in:

$$N_A \approx 2\pi \cdot \left(\frac{1+\lambda}{2\lambda}\right)^2 \cdot \int_0^{\alpha_{max}} \sin(\alpha) d\alpha$$

$$\approx 2\pi \cdot \left(\frac{1+\lambda}{2\lambda}\right)^2 \cdot [1 - \cos(\alpha_{max})] \tag{31}$$

The total number of particles N_{tot}, which covers a bubble completely, follows from Eq. 31 after substitution of $\alpha_{max} = \pi$. Then, the fraction ζ of the bubble surface area covered by particles can be derived from Eq. 31:

$$\zeta = \frac{N_A}{N_{tot}} = \frac{1}{2} \cdot \{1 - \cos(\alpha_{max})\} \tag{32}$$

If the downward force, exerted on the lowest particle by the monolayer of particles, is equal to the apparent weight of a fraction ψ of the adhering monolayer, we may state that Eqs. 27 and 31 lead to:

$$\psi = \frac{(n_A)_{max}}{N_A} = \frac{\lambda}{4(1+\lambda)} \cdot \left\{\frac{2\alpha_{max} - \sin(2\alpha_{max})}{1 - \cos(\alpha_{max})}\right\} \tag{33}$$

where $0 \leq \psi \leq \pi\lambda/[4(1+\lambda)]$, if $0 \leq \alpha_{max} \leq \pi$.

Effect of curvatures of particle and bubble surfaces on θ

According to the extended Young-Dupré equation (Schulze, 1984):

Table 1. Relevant Physical Properties of Catalyst Particles Used

Catalyst	ρ_{SK} kg·m^{-3}	$V_p \cdot 10^3$ m^3·kg^{-1}	$A \cdot 10^{-3}$ m^2·kg^{-1}	$\rho_P^{(*)}$ kg·m^{-3}
Pd/C (10 wt. %)	2,280	1.839	883	$439+0.807\rho_L$
Pd/Al_2O_3 (10 wt. %)	3,340	0.250	158	$1820+0.455\rho_L$
$Pd/BaSO_4$ (10 wt. %)	4,370	0.193	21	$2371+0.458\rho_L$

(*)Calculated from: $\rho_P = \frac{1+V_p\rho_L}{1+V_p\rho_{SK}} \cdot \rho_{SK}$

$$\sigma_{SG} - \sigma_{SL} = \sigma_{LG}\cos(\theta_E) - \frac{\kappa}{r} \tag{34}$$

an effective contact angle θ_E is obtained if the value of the term κ/r is significant compared with the value of $\sigma_{LG}\cdot\cos(\theta_E)$. This may be the case for small values of the radius of the three-phase contact ring, for example, $r \leq 10^{-7}$ m (see Figure 2). For the three-phase systems investigated, the values of r indeed are in the order of 10^{-7} m, and as a result the effect of the term κ/r may not be neglected. It has to be noted that κ has been called "linear tension" by Langmuir (1933). In more recent literature (Scheludko, 1976; Schulze 1984), however, the term κ/r, which has the same dimension as a surface tension, is mentioned "linear tension," while κ is indicated as the "line energy." If $1/r \to 0$, the contact angle $\theta_E \to \theta_0$, and Eq. 34 is reduced to the well-known Young equation:

$$\sigma_{SG} - \sigma_{SL} = \sigma_{LG}\cos(\theta_0) \tag{35}$$

Combination of Eqs. 34 and 35 results in:

$$\cos(\theta_E) = \cos(\theta_0) + \frac{\kappa}{\sigma_{LG} r} \tag{36}$$

The value of r in the extended Young-Dupré equation can be approximated by (see Figure 2):

$$r = R_P \sin(\varphi_m) \approx \frac{R_P\theta_E}{2(1+\lambda)} \tag{37}$$

where φ_m is obtained from Eq. 10.

Table 2. Experimental Results

Type of Catalyst Particle	R_B mm	R_P μm	$\alpha_{max}^{(*)}$ Degree	$\theta_E^{(**)}$ Degree
Air Bubbles				
10 wt. % Pd/C ($\theta_0 = 2.2°$)	0.36	8	109 ± 5	1.23 ± 0.04
	0.46	8	106 ± 8	1.33 ± 0.08
	0.56	8	92 ± 8	1.29 ± 0.11
	0.35	13	109 ± 11	1.62 ± 0.11
	0.46	13	101 ± 10	1.71 ± 0.16
	0.55	13	102 ± 8	1.91 ± 0.14
	0.36	18	107 ± 11	1.87 ± 0.17
	0.45	18	100 ± 13	2.02 ± 0.24
	0.55	18	93 ± 8	2.07 ± 0.23
	0.46	23	84 ± 6	2.05 ± 0.14
	0.54	23	82 ± 8	2.13 ± 0.26
10 wt. % Pd/Al_2O_3 ($\theta_0 = 5.3°$)	0.35	10	113 ± 10	3.30 ± 0.21
	0.45	10	111 ± 8	3.60 ± 0.20
	0.56	10	110 ± 5	4.03 ± 0.17
	0.35	22	117 ± 8	5.20 ± 0.20
	0.45	22	93 ± 8	4.81 ± 0.54
	0.55	22	80 ± 12	4.59 ± 0.81
	0.35	28	84 ± 8	4.33 ± 0.48
	0.45	28	82 ± 12	5.00 ± 0.84
	0.55	28	73 ± 8	4.83 ± 0.80
	0.45	39	63 ± 9	4.96 ± 0.72
	0.55	39	68 ± 9	5.07 ± 0.66
10 wt. % $Pd/BaSO_4$ ($\theta_0 = 11.3°$)	0.37	30	104 ± 12	7.14 ± 0.99
	0.45	30	100 ± 8	7.09 ± 0.49
	0.55	30	103 ± 7	8.20 ± 0.40
	0.45	38	107 ± 8	9.14 ± 0.56
	0.55	38	95 ± 12	8.51 ± 0.66

Type of Catalyst Particle	R_B/mm	R_P/μm	α_{max}^{*}/Degree
Hydrogen Bubbles			
10 wt. % Pd/C	0.35, 0.45, 0.55	8, 13, 18, 23	Completely Covered
10 wt. % Pd/Al_2O_3	0.35, 0.45, 0.55	10, 22, 28, 39	Zero Coverage
10 wt. % $Pd/BaSO_4$	0.35, 0.45, 0.55	30, 38	≤20 (Clusters)

(*)Average values of at least eight experiments.
(**)Calculated with Eqs. 23 and 24.

The effect of the curvatures of the particle and bubble surfaces is incorporated in the radius r of the three-phase contact ring. From Eq. 36, it is obtained that for a given G/L/S system, the value of θ_E will *decrease* with *decreasing* values of r. This means that for the range of particle and bubble radii applied in this article, the adhesion of particles to a gas bubble is governed by an effective contact angle θ_E.

The value of the G/L/S system properties θ_0 and κ can be found by plotting the value of $\cos(\theta_E)$ against $1/r$. If a linear relationship is found, the value of θ_0 is obtained by extrapolation of $1/r \rightarrow 0$ and the value of κ from the slope of the line. The values of θ_0 and κ thus obtained are physical properties of the G/L/S system. They are independent of the curvatures of the interfaces.

Equipment and Materials

The experiments are performed with an apparatus that consists of two separated cylindrical cells (see Figure 7). The outer cell is used to thermostat the inner cell containing a stagnant liquid and a small glass cup, placed on a stainless steel holder. A needle can be introduced into this inner cell via two rubber septums. The cylinder between the septums contains either air or hydrogen.

The commercially available catalyst particles used are 10 wt. % Pd/C, 10 wt. % Pd/Al_2O_3, and 10 wt. % $Pd/BaSO_4$ (Fluka Chemie AG), of which some relevant physical properties are given in Table 1. Samples of different particle size are obtained using ASTM-E11 standard sieves. The average particle size and the particle size distribution of each sample are determined with a Coulter Counter. The Pd/Al_2O_3 and $Pd/BaSO_4$ catalyst particles are approximately spherical with a relatively smooth surface; and the Pd/C catalyst particles have rather irregular shapes.

Commercially available catalysts are used without performing any pretreatment such as grinding, to prevent unpredictable effects on the experimental results. With the BPU method, the particle-to-bubble adhesion is characterized under conditions that may be encountered in such processes as flotation processes and three-phase reacting systems.

When hydrogen (Ultra High Purity, from Ucar) is applied, the particles and liquid are saturated with hydrogen at 1 atm before they are used for the adhesion experiments. A similar procedure is applied if air is used as the gas in the system. All experiments are performed in double-distilled water at 303 K and atmospheric pressure.

Procedure

Figure 7 shows the apparatus, in which the inner cell (1) is filled with gas-saturated liquid and the cylinder (7) is filled with the required gas. The needle of a gastight syringe is pierced through the upper septum (6) and the syringe is flushed at least five times with the gas. The syringe is then again filled with the gas and the needle is pierced through the lowest septum (6). A bubble is formed on the tip of the needle, which is positioned just above the bottom of the glass cup (12). A gas-saturated concentrated suspension of catalyst particles is added through opening (9) until the bubble is completely immersed under a small layer of sedimented catalyst particles.

This method is a modification of the procedure used by Wimmers (1987, 1988). The bubble is *slowly*, say in about 30 seconds, pulled out of this small sedimented layer on the bottom of the small glass cup. In this way, a bubble, partially covered by adhering particles, is obtained. An enlarged image of this bubble with adhering particles is achieved by projecting it with the aid of an optical system on a screen. From this enlarged image, the angle of bubble-surface coverage and the bubble diameter are obtained. The maximum angle of coverage α_{max} is determined using systems that consist of air-water-catalyst particles and hydrogen-water-catalyst particles for different particle and bubble sizes, obeying the condition $\lambda < 0.10$.

Table 3. Values of θ_0 and κ(*)

Type of Catalyst Particle	θ_0 Degree	$\kappa \cdot 10^{11}$ N
10 wt. % Pd/C	2.2±0.08	0.29± 0.03
10 wt. % Pd/Al_2O_3	5.3±0.21	4.93± 0.69
10 wt. % $Pd/BaSO_4$	11.3±0.20	142 ±22.83

(*)The values refer to the systems consisting of air, water and three different types of catalyst particles.

Results

The measured angles of bubble-surface coverage α_{max} for the above-mentioned systems and for various particle and bubble radii are listed in Table 2. In the experiments where an air bubble is used, it is observed that the adhering particle layer is a monolayer; so that the PBA model consisting of Eqs. 23 and 24, or Eq. 28 may be applied.

The experimental results show that α_{max} depends on the modified Eötvös number *Eo* of the system, the ratio λ of the particle and bubble radii, and the G/L/S contact angle. In a previous section, it was shown that the particle-to-bubble adhesion is governed by an effective contact angle θ_E which is smaller than the contact angle θ_0 occurring at a straight G/L/S contact line (see Figure 1). According to Eq. 36, the values of $\cos(\theta_E)$, obtained from Eqs. 23 and 24 and the measured values of α_{max}, *Eo* and λ against the curvature $1/r$ of the G/L/S contact ring calculated with Eq. 37, will result in a straight line for each of the different types of catalyst particles. For three of the systems investigated, the values of $\cos(\theta_0)$ and κ were obtained from a best-fit procedure applied to the experimental data presented in Figures 8a–8c. The values of θ_0 and κ thus obtained for the air-water-catalysts systems Pd/C, Pd/Al_2O_3 and $Pd/BaSO_4$ are presented in Table 3.

From Figures 8a–8c and Table 3, it is found that the value of κ is: independent of the curvatures of the particle and bubble surfaces; and different for G/L/S systems with different θ_0 values. These results agree with those of Schulze (1984), who states that κ values, which are affected by the contact angle θ_0, are in the order of 10^{-11} N to 10^{-10} N.

When hydrogen bubbles in water are applied, all types of catalyst particles agglomerate. They form relatively large clusters due to the formation of a hydrophobic particle surface which is created after adsorption of hydrogen on the catalyst surface. In experiments with Pd/C particles and *hydrogen* bubbles in water, the bubble was always completely covered with clusters of particles. In the experiments with Pd/Al_2O_3 particles and $Pd/BaSO_4$ particles and *hydrogen* bubbles in water, the angle of bubble-surface coverage was almost zero.

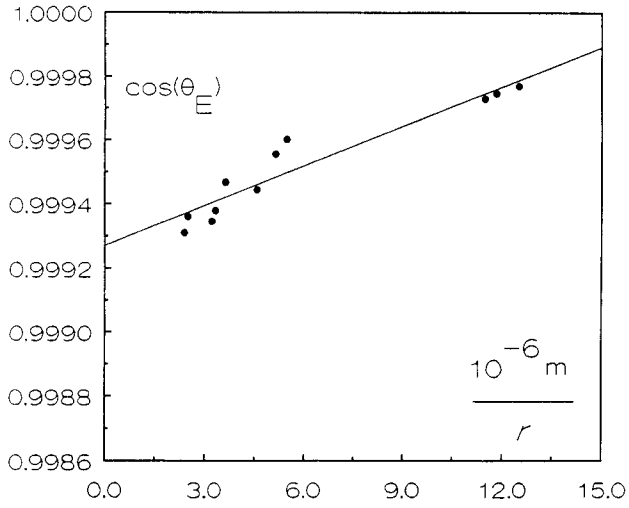

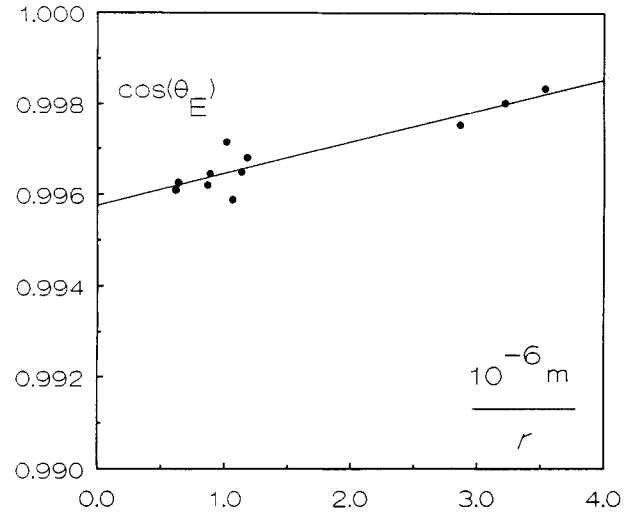

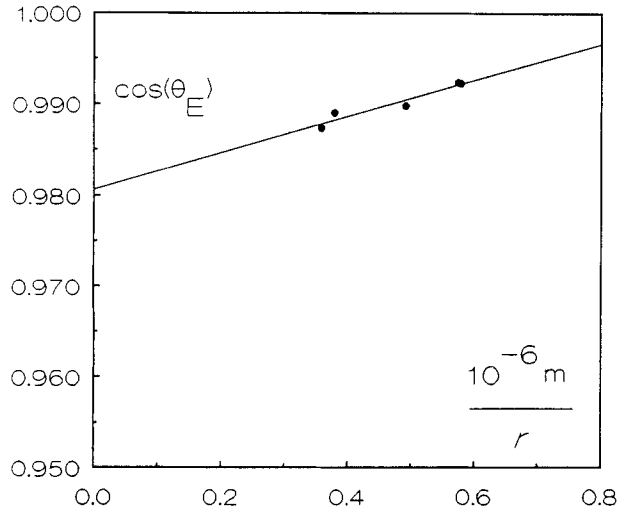

Figure 8. Value of $\cos(\theta_E)$ vs. $1/r$.

(a). Air-water-Pd/C system
(b). Air-water-Pd/Al_2O_3 system
(c). Air-water-Pd/$BaSO_4$ system

The value of θ_E is calculated with Eqs. 23 and 24 using the measured values of α_{max}.

In this case, clusters of particles are formed and nearly no particle-to-bubble adhesion occurs.

Discussion

Effect of adsorbed gas

A hydrophobic catalyst surface is created after *hydrogen* adsorption on the catalyst surface. In polar liquids, growing hydrophobicity of the catalyst particle surface does not only increase the value of the contact angle and consequently the particle-to-bubble *adhesion*, but also the particle-to-particle *cohesion*, resulting in the formation of clusters. Large clusters of high-density particles are unable to adhere to a hydrogen bubble in water, as is observed for Pd/Al_2O_3 and Pd/$BaSO_4$. For the low-density Pd/C particles, however, a hydrogen bubble in water is completely covered with particles because $\theta_E > \theta^*$ (see Eq. 29). Hydrogen bubbles in water have the following tendency: Pd/C particles show a particle-to-bubble adhesion which dominates the particle-to-particle cohesion; and Pd/Al_2O_3 and Pd/$BaSO_4$ show a particle-to-particle cohesion which dominates the particle-to-bubble adhesion.

Comparison with existing methods

In literature, no methods could be found for determining contact angles of *porous* particles with $\theta < 15°$. Existing methods for nonporous particles are inaccurate for measuring contact angles $\theta < 15°$. Therefore, the results presented here cannot be compared with those from literature. However, the fact that experimentally a linear relationship is obtained between $\cos(\theta_E)$ and $1/r$, which agrees with the extended Young-Dupré equation, contributes to the validation of the present method. The BPU method not only includes the effect of the curvatures of the interfaces, but is also closely related to the conditions occurring during flotation and in slurry reactors.

Conclusions

In a G/L/S slurry the particle-to-bubble adhesion depends on: the modified Eötvös number *Eo* of the system; the ratio λ of the radii of particle and bubble; and the effective solid-liquid-gas contact angle θ_E. The cosine of the effective contact angle θ_E is a linear function of the curvature $1/r$ of the G/L/S contact ring. The contact angle θ_0 and the "line energy" κ are physical properties of a G/L/S system, which are independent of the curvature of the G/L/S contact ring. The G/L/S contact angle can be affected by the type of gas adsorbed on the surface of the catalyst particles.

The PBA model, represented by Eqs. 23 and 24, or by Eq. 28, may be applied to the investigated systems consisting of air/water/catalyst particles, because it has appeared that under equilibrium conditions, a *monolayer* of catalyst particles adheres to the air bubble in water. For the systems air/water/catalyst particles, the following values of the contact angle θ_0 are found: $\theta_0 = 2.2°$ for Pd/C; $\theta_0 = 5.3°$ for Pd/Al_2O_3; and $\theta_0 = 11.3°$ for Pd/$BaSO_4$. A monolayer of catalyst particles will cover the bubble surface completely if $\theta_E \geq \theta^*$, where θ^* can be obtained from Eq. 29.

For hydrogen bubbles in water, the Pd/C particles show a particle-to-bubble *adhesion* which dominates the particle-to-particle *cohesion*; and the Pd/C particles can cover the hydrogen bubble completely. The Pd/Al_2O_3 and Pd/$BaSO_4$ par-

ticles for these bubbles show a particle-to-particle *cohesion* which dominates the particle-to-bubble *adhesion*, resulting in the formation of large clusters which are unable to adhere to a hydrogen bubble in water.

Acknowledgment

The authors wish to thank Mrs. M. Mittelmeyer-Hazeleger of the University of Amsterdam for determining the physical properties of the catalyst particles and Mr. G. Bierman for performing part of the experiments.

Notation

A = BET-specific surface area of catalyst particles, $m^2 \cdot kg^{-1}$
Eo = modified Eötvös number $= (\rho_P - \rho_L) g R_P^2 / \sigma_{LG})$, 1
F = force, N
F_A = apparent weight of a particle in a liquid, N
F_{AC} = apparent weight of a cluster consisting of n_C equal-sized spherical particles in a liquid, N
$F_{i,j}$ = component of the apparent weight of a particle positioned under an angle $i \cdot \Delta\alpha$ (Figure 4), N
F_i^* = contribution of all the particles positioned on parallel i of a globe with radius $R_B + R_P$ to the downward force exerted on the lowest particle, N
F^* = total downward force exerted on the lowest particle by all other particles of the adhering monolayer, N
F_C = capillary force, N
F_P = force due to the capillary pressure in the gas bubble, N
g = acceleration due to gravity ($g = 9.81\ m \cdot s^{-2}$), $m \cdot s^{-2}$
n = maximum number of parallels with adhering particles, 1
$(n_A)_{max}$ = maximum number, defined in Eq. 25, 1
n_C = number of equally sized particles in a cluster (Figure 2), 1
$(n_C)_{max}$ = maximum value of n_C, 1
N_A = total number of adhering particles at the gas-bubble surface, 1
N_i = number of adhering particles positioned on parallel i of the globe with radius $R_B + R_P$, 1
N_{tot} = total number of adhering particles in a monolayer covering the bubble completely, 1
$P_{i,j}$ = intersection point of parallel i and meridian j of the globe with radius $R_B + R_P$, 1
P_σ = capillary pressure in a gas bubble, $N \cdot m^{-2}$
r = radius of the three-phase contact ring (Figure 2), m
R_B = radius of a gas bubble, m
R_P = radius of a catalyst particle, m
V_P = specific pore volume of a particle, $m^3 \cdot kg^{-1}$

Greek letters

$\Delta\alpha$ = angle between centers of two neighboring particles adhering to a gas bubble (Figure 4), rad
$i \cdot \Delta\alpha$ = angle indicating the position of a particle at a gas bubble surface (Figure 4), rad
α_{max} = measured maximum angle of bubble-surface coverage, rad
ζ = fraction of the gas-bubble surface area covered by catalyst particles (Eq. 32), 1
θ = G/L/S contact angle, rad
θ^* = minimum value of θ required for complete bubble-surface coverage, rad
θ_E = effective G/L/S contact angle, rad
θ_0 = contact angle at zero curvature of the contact line, rad
κ = line energy, N
λ = ratio of particle and bubble radii ($\lambda = R_P/R_B$), 1
ρ_G = density of the gas phase, $kg \cdot m^{-3}$
ρ_L = density of the liquid phase, $kg \cdot m^{-3}$
ρ_P = density of the particle with pores filled with liquid, $kg \cdot m^{-3}$
ρ_{SK} = density of the solid part of a dry catalyst particle, $kg \cdot m^{-3}$
σ_{LG} = static surface tension of a gas-liquid interface, $Pa \cdot m$
σ_{SG} = surface tension of solid-gas interface, $Pa \cdot m$
σ_{SL} = surface tension of solid-liquid interface, $Pa \cdot m$
φ = angle characterizing the immersion depth of a particle, rad
φ_m = minimum value of φ_s before the particle is released from the gas bubble where $n_C = (n_C)_{max}$, rad
φ_s = angle characterizing the immersion depth of a particle under static conditions, rad
ψ = physical quantity defined in Eq. 33, 1

Literature Cited

Ayala, R. E., E. Z. Casassa, and G. D. Parfitt, "A Study of the Applicability of the Capillar Rise of Aqueous Solutions in the Measurement of Contact Angles in Powder Systems," *Powder Technol.*, **51**, 3 (1987).

Heertjes, P. M., and N. W. F. Kossen, "Measuring the Contact Angles of Powder-Liquid Systems," *Powder Technol.*, **1**, 33 (1967).

Kossen, N. W. F., and P. M. Heertjes, "The Determination of the Contact Angle for Systems with a Powder," *Chem. Eng. Sci.*, **20**, 593 (1965).

Langmuir, I., "Oil Lenses on Water and the Nature of Monomolecular Expanded Films," *J. Chem. Phys.*, **1**, 756 (1933).

Lindner, D., and M. Werner, and A. Schumpe, "Hydrogen Transfer in Slurries of Carbon Supported Catalyst (HPO Process)," *AIChE J.*, **34**, 1691 (1988).

Neumann, A. W., and R. J. Good, "Techniques of Measuring Contact Angles," *Surf. Colloid. Sci.*, **11**, 31 (1979).

Scheludko, A., B. V. Toshev, and D. T. Bojadjiev, "Attachment of Particles to a Liquid Surface (Capillary Theory of Flotation)," *J. Chem. Soc. Trans. Farad.*, **72**, 2815 (1976).

Schulze, H. J., "Physico-Chemical Elementary Processes in Flotation," *Developments in Mineral Processing*, **4**, Elsevier Science, New York (1984).

Sell, P. J., A. W. Neumann, "Die Oberflächenspannung fester Körper," *Angew. Chem.*, **6**, 321 (1966).

Sell, P. J., "Randwinkelmessungen an pulverförmigen Stoffen," *Phys. Chem. Anwendungstech.*, **3**, 23 (1972).

Wimmers, O. J., "The Enhancement of Gas-Absorption by a Heterogeneously Catalysed Chemical Reaction," PhD Thesis, Univ. of Amsterdam (1987).

Wimmers, O. J., and J. M. H. Fortuin, "The Use of Adhesion of Catalyst Particles to Gas Bubbles to Achieve Enhancement of Gas Absorption in Slurry Reactors: I. Investigation of Particle-to-Bubble Adhesion Using the Bubble Pick-Up Method," *Chem. Eng. Sci.*, **43**, 303 (1988).

Manuscript received Jan. 14, 1991, and revision received Aug. 28, 1991.